

DeepMRI: Exploiting deep residual network for fast parallel MR imaging with complex convolution

Shanshan wang¹, Huitao Cheng¹, Taohui Xiao¹, Ziwen Ke¹, Leslie Ying², Xin Liu¹, Hairong
Zheng^{1,*}, Dong Liang^{1,*}

¹Paul C. Lauterbur Research Centre for Biomedical Imaging, Shenzhen Institutes of Advanced
Technology, Shenzhen, Guangdong 518055, China

²Department of Biomedical Engineering and Department of Electrical Engineering, University
at Buffalo, The State University of New York, Buffalo, New York 14260, USA

***Correspondence to:**

Dong Liang, Ph.D., Hairong Zheng, PhD,

Paul C. Lauterbur Research Centre for Biomedical Imaging

Institute of Biomedical and Health Engineering

Shenzhen Institutes of Advanced Technology

Chinese Academy of Sciences, Shenzhen, Guangdong, China, 518055

Tel: (86) 755-86392243

Fax: (86) 755-86392299

Email: dong.liang@siat.ac.cn, hr,zheng@siat.ac.cn

Running head: DeepMRI: Exploiting deep residual network for fast parallel MR imaging with
complex convolution

Word count: 4980

Abstract

Purpose: To accelerate MR scan, this paper incorporates deep learning into fast MR imaging by exploiting deep residual neural network with complex convolution for parallel MR image (DeepMRI) reconstruction from undersampled multi-coil measurements.

Methods: DeepMRI draws and utilizes prior knowledge from a large number of existing fully-sampled multi-coil measurements for accurate online fast imaging. It designs and trains an off-line deep residual convolutional neural network to describe the mapping relationship between the MR images reconstructed from the undersampled and fully-sampled k-space data. Specifically, complex convolution was proposed to consider the intercorrelation between the real and imaginary parts. Furthermore, both k-space data fidelity and image space proximity are considered for the network training.

Results: The evaluations on in vivo datasets show that the proposed DeepMRI has strong capability in capturing image information that are lost in the zero-filled MR images. The comparison with the classical SPIRiT and L1-SPIRiT has demonstrated that DeepMRI can reconstruct MR images more accurately.

Conclusion: Deep learning with complex convolution can be used to learn valuable prior knowledge from off-line training datasets and then perform high-quality online reconstruction from undersampled multi-coil data.

Key words: Deep learning, convolutional neural network, fast MR imaging, prior knowledge, parallel imaging

Introduction

Parallel imaging has been an essential technique to accelerate MR scan. With the utilization of spatial sensitivity of multiple coils in conjunction with gradient encoding, it shortens the imaging time by reducing the amount of acquired data needed for MR image reconstruction. Typical examples include sensitivity encoding (SENSE) [1], simultaneous acquisition of spatial harmonics (SMASH) [2], generalized auto-calibrating partially parallel acquisitions (GRAPPA) [3], iterative self-consistent parallel imaging reconstruction (SPRiT) [4], parallel imaging using eigenvector maps (referred to as ESPIRiT) [5] and so on [6-9].

Besides exploring the physical multi-coil properties, many endeavors have been made to use signal processing in MR image reconstruction. Specifically, diverse prior information has been exploited and incorporated into the reconstruction formulation as regularizations. Among them, one representative effort focuses on compressed sensing, which utilizes incoherent undersampling and image sparsity for fast MR imaging. For example, wavelet [10], total variation [11, 12], joint total variation [13], nonlocal total variation [14] and dictionary learning [15] are used to promote the sparsity of the to-be-reconstructed MR images for high accelerations. In addition to sparsity, there are also other priors under consideration, such as partial separable function [16], low-rank [17-20], statistics distribution regularization [21], manifold fitting [22-24], GS model [25] and so on [26, 27].

Nevertheless, most traditional parallel imaging techniques have only exploited prior information either directly from the to-be-reconstructed images or with very few reference images involved. Based on the fact that the enormous images acquired every day share similar organ structures and anatomic information, we previously proposed to learn an off-line convolutional neural network (CNN) prior model [28, 29] to aid online single-coil MR reconstruction. Meanwhile and thereafter, different deep learning approaches have been developed for fast MR imaging [30-40]. For example, there are model based unrolling methods, such as VN-Net [30, 31], and ADMM-Net [32], and end-to-end learning methods like AUTOMAP [33], U-NET [34], and so on so forth [35-40]. There is also a work using multilayer perceptron (MLP) to assist parallel MR imaging [41]. While MLP is a fully-connected network

which has lots of parameters, CNN assumes local connections between previous and subsequent layers and thereby reduces the number of parameters. In addition, the wide application of CNN has shown its strong capability in automatic feature extraction, correlation exploration and nonlinear correlation description [31]. Motivated by the fact that the multi-coil data describe the same anatomic structure, we exploited CNN and extended our previous single-coil CNN MR imaging method to multi-coil parallel and different imaging tasks [42] [43]. Nevertheless, our previous work hasn't considered the k-space correlations but just the image space mapping and only with 1D undersampling pattern. Furthermore, all the operations haven't considered the correlation between the real and imaginary part. We also realize that when researchers try to keep the complex nature of MR images [43], the essence still treats real and imaginary parts independently for the convolution.

Based on these observations, this paper exploits deep residual neural network with complex convolution for parallel MR image (DeepMRI) reconstruction from undersampled multi-coil measurements. Specifically, we introduce a complex convolution by simulating complex arithmetic using real-valued arithmetic internally. It considers the correlations between the real and imaginary parts. Complex weight initiation strategies are provided. In addition, both k-space data fidelity and image space proximity have been considered for the network training to draw more valuable knowledge from available big datasets. To avoid the vanishing gradient problems of network training, residual connections are also adopted. The learned network then is used to assist online parallel MR imaging. We investigate the performance of the proposed method with respect to quite a few representative 1D and 2D undersampling patterns. And it has been tested on a series of in vivo datasets and compared to the classical parallel image reconstruction methods such as SPIRiT, and the compressed sensing based parallel imaging method L1-SPIRiT.

Methods

Review of Convolutional Neural Network

For a complete illustration of the proposed method, we firstly provide a brief review of the convolutional neural network (CNN). An L-layer CNN $y = C(x, \theta)$ can be described as follows

$$\begin{cases} C_0 = X \\ C_l = \sigma_l(\Omega_l * C_{l-1} + b_l) \\ C_L = \Omega_L * C_{L-1} + b_L \end{cases} \quad l = 1, 2, \dots, L-1 \quad (1)$$

where Ω_l denotes the convolution operator of size $FW_l \times FH_l \times K_{l-1} \times K_l$ and b_l is the K_l dimensional bias with its element associated with a filter. The CNN output y is C_L , the output of the final layer. Here, K_{l-1} is the number of the feature maps extracted at the layer $l-1$, $FW_l \times FH_l$ means the filter size and K_l is the number of filters at layer l , and σ_l means the nonlinear mapping operator. Eq. 1 could be regarded as the forward pass of the CNN training, where the convolution operator is used to extract the features and σ_l calculates the nonlinear activation.

Besides the forward pass, the backward propagation updates the network parameters by calculating the backward gradients. Specifically, given the training pairs (x, y) , the backward propagation is to update $\theta = \{(\Omega_1, b_1), \dots, (\Omega_l, b_l), \dots, (\Omega_L, b_L)\}$, which minimizes a cost function

$$\hat{\theta} = \arg \min_{\theta} J(x, y) \quad (2)$$

where $J(x, y)$ is the cost function determined by the specific problem. Once $\hat{\theta}$ is obtained, it can be used for online tasks to predict the target $y = C(x, \hat{\theta})$, where x is now the online test input.

Review of our previous work

In our previous work, we proposed to apply deep learning to single-channel MR image reconstruction. Its framework consists of two main parts: offline training and online imaging. For offline training, there are two major ingredients namely the network design and the processing of big datasets for training samples. As can be seen from [28], we used CNN as the deep learning tool to draw prior information from the sub-image patches extracted from the single-coil data samples. The overall training formula can be described as follows

$$\theta = \arg \min_{\theta} \sum_{t=1}^T \sum_{n=1}^N \|C(x_{t,n}; \theta) - y_{t,n}\|_2^2 \quad (3)$$

where $x_{t,n}$ presents the t -th patch in the n -th zero-filled MR image from undersampled data, $y_{t,n}$ is the corresponding groundtruth (so-called ‘label’ in deep learning) patch reconstructed from the full data, T means the total number of patches extracted from each image and N represents the total number of images in the training dataset.

For online imaging, besides direct online prediction of images with the network, we also provide two options for integrating the network prediction with the regularization method. One is the two-phase reconstruction integration, where the first phase is to predict an image from the undersampled data with the learned network $y_{\text{initial}} = C(x; \theta)$ and the second phase is to use the prediction y_{initial} as the initialization for the iterative reconstruction $\hat{y} = \arg \min_y \{R(y) + \lambda \|\hat{x} - F_u y\|_2^2\}$, where $\|x - F_u y\|_2^2$ is the data fidelity term and $R(y)$ is the regularization term.

The other is to adopt the image generated by the network as a reference image and use it as an additional regularization term. The formulation can be described as

$$\hat{y} = \arg \min_y \{R(y) + \lambda \|\hat{x} - F_u y\|_2^2 + \alpha \|C(x; \theta) - y\|_2^2\} \quad (4)$$

The proposed method

This work proposed a DeepMRI model to identify the undersampling relationship between the multi-coil undersampled MR data and the fully sampled MR image. Both k-space data fidelity and image space proximity have been considered for the network training. Figure 1 shows the architecture of the proposed network for parallel imaging. The input of the network is the multi-channel image transformed from zero-filled undersampled k-space data. The label is the multi-channel reconstructed image from the fully sampled dataset. Different from the single-coil reconstruction, the input and output directly include all the channels, which will be discussed in the later session. In the middle section of the network, the acquired undersampled k-space data is used to keep data fidelity. As can be seen from the figure, the network alternates between a sub-CNN and a data-consistency layer.

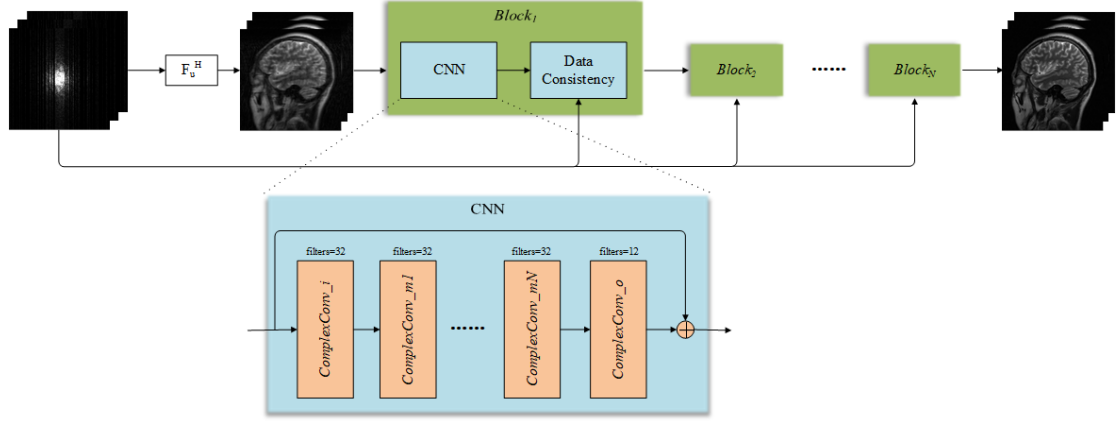


FIG. 1. The architecture of the DeepMRI for parallel imaging.

The mean absolute error (MAE) between the ground truth and the network output was used as the training loss function, which can be described as follows

$$\hat{\theta} = \arg \min_{\theta} J(x, y) \text{ where } J = \frac{1}{M} \sum_{m=1}^M \|C(x_m; \theta) - y_m\| \quad (5)$$

where x_m denotes the m-th multi-channel input image from zero-filled k-space data, y_m means the corresponding fully-sampled multi-channel groundtruth, and M means the number of images in a batch.

Data Consistency in k-space

Besides enforcing the closeness between the image generated by the network with the groundtruth, we also promote k-space completion by a data fidelity layer as shown in each block. Let f_l denote the Fourier encoding of the multi-channel image reconstructed by the learned network at layer l , i.e. $f_{l,j} = \mathbb{F}y_{l,j} = \mathbb{F}C_l(x; \theta)$. $f_{l,j}(k)$ represents the pixel value of the k-space at the index k of the j -th channel. To make the reconstruction more accurate, the acquired undersampled data can be projected onto the k-space transformed from the reconstructed image, which can be described as

$$f_{l,j}(k) = \begin{cases} y_{l,j}(k) & \text{if } k \notin S \\ \frac{y_{l,j}(k) + \lambda f_{0,j}(k)}{1 + \lambda} & \text{if } k \in S \end{cases} \quad (6)$$

where $f_{0,j}$ denotes the zero-filled undersampled k-space data and S is the set of sampled locations. Then the final multi-channel image is reconstructed with the inverse Fourier transform of this k-space data $y_{l,j} = \mathbb{F}^H f_{l,j}$.

Complex Convolution

Because of the complex nature of MR image, it is essential to deal with complex-valued data using deep residual convolutional neural network. The majority of the current CNNs for MR reconstruction treat a complex-valued MR image as two-channeled real-valued data, with the real and imaginary component concatenated. Here, we deal with MR images in the same way, but what is different is that we introduce a complex convolution, which simulates complex arithmetic using real-valued arithmetic internally.

To perform the equivalent of a traditional real-valued 2D convolution in the complex domain, we convolve the complex filter matrix $\Omega = \Omega_{real} + i\Omega_{imagi}$ with a complex image input vector $u = u_{real} + iu_{imagi}$, where Ω_{real} and Ω_{imagi} are real-valued matrices and u_{real} and u_{imagi} are real vector since we are simulating complex arithmetic using real-valued entities. Since convolution operator is distributive, we have

$$\Omega * u = (\Omega_{real} * u_{real} - \Omega_{imagi} * u_{imagi}) + i(\Omega_{real} * u_{imagi} + \Omega_{imagi} * u_{real}) \quad (7)$$

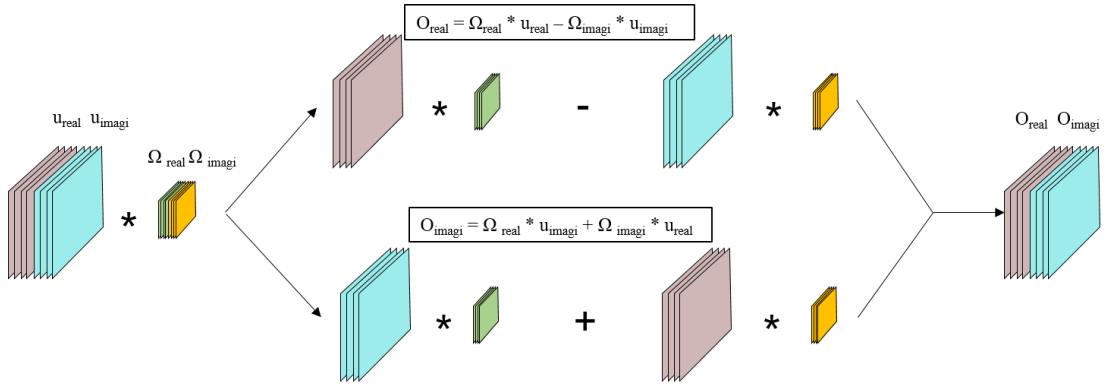


FIG. 2. The proposed complex convolution

For neural network learning, proper initialization is critical in reducing the risk of vanishing gradients especially in the case when batch normalization is not adopted. A complex weight has a polar form as well as a rectangular form

$$\Omega = |\Omega|e^{i\theta} = \Omega_{real} + i\Omega_{imagi} = |\Omega|\cos\theta + i|\Omega|\sin\theta \quad (8)$$

where θ and $|\Omega|$ are respectively the phase and magnitude of Ω .

According to Chi-distribution with two degrees of freedom, the magnitude of the complex weight is Rayleigh-distributed assuming that the real and imaginary components are independently and identically distributed Gaussian with equal variance and zero mean.

Therefore, it is reasonable to initialize the magnitude of the complex parameter Ω using the Rayleigh distribution. We then use the uniform distribution between $-\pi$ and π to initialize the phase of Ω . With the magnitude and phase multiplied, we perform the complete initialization of the complex parameters.

Online reconstruction

Consider the undersampled multi-coil raw k-space data as

$$z = F_p v \quad (9)$$

where $F_p = PF$, v means the concatenation of multi-coil sensitivity encoded images v_j for parallel imaging scenario $v = [v_1; v_2; \dots; v_j \dots; v_J]$, P is a circular diagonal matrix representing the undersampling mask. F denotes the normalized full Fourier encoding matrix such that $F^H F = I$; superscript H means the Hermitian transpose operation. Correspondingly, the zero-filled reconstruction can be described as

$$x = F_p^H F_p v \quad (10)$$

With a data consistency layer following every residual block, we can directly obtain the multi-coil reconstruction by

$$y_{multi} = C(x; \hat{\theta}) \quad (11)$$

where $\hat{\theta}$ denotes the well-trained weights of our DeepMRI model. For display the final result, we could use adaptive coil combination method [44] or use the square root of the sum-of-squares.

Dataset

The training dataset consists of over 3000 fully sampled MR brain images we collected from 3T scanner (SIEMENS MANGETOM Trio Tim) with a 12-channel head coil. The images are of a great diversity including axial, sagittal, horizontal images with different contrasts such as T1, T2 and PD, and images of different sizes. Informed consents were obtained from the imaging subject in compliance with the Institutional Review Board policy. We normalize the multi-channel data to have a maximum magnitude value of 1. Undersampled measurements were retrospectively obtained using the pre-defined undersampling masks. Deep learning depends on big datasets, which are hard to obtain for medical images. Therefore, data augmentation including rigid transformation is adopted to improve the network performance and avoid overfitting. Specifically, for each image, we apply rotation of $[0, 2\pi)$, reflection along x-axis and y-axis. In this way, we create 8 augmented data per image.

Network Architecture Configurations and implementation setup

We used a minibatch size 4 for the training of the proposed network. Significantly, all training was performed with whole images instead of patches for promoting k-space completion via data consistency layers and better capturing FOV structures. With respect to the optimizer, Adam method was used with $\beta_1 = 0.9$, $\beta_2 = 0.999$ and initial learning rate = 0.0001. The training processes were implemented on an Ubuntu 14.04 LTS (64-bit) operating system equipped with Graphics Quadro K40c in the open framework tensorflow. The online imaging processes were implemented on an Ubuntu 14.04 LTS (64-bit) operating system equipped with 128GB RAM and Intel Xeon(R) CPU E5-2660 v3 in Matlab 2015b.

Undersampling Masks

Three different types of undersampling pattern was tested, including 1D variable density random, 2D Poisson disc and 2D random. For 2D Poisson disc mask, 3x, 5x, and 10x acceleration were simulated by retaining 33%, 20% and 10% raw k-space data. For both 1D and 2D random masks, 3x and 4x acceleration was simulated.

Results

Impact of complex convolution

To demonstrate the impact of complex convolution on the reconstruction, we trained two networks, between which the only difference was whether complex convolution was adopted or not. It is noted that the networks for this experiment consist of 5 blocks, and each block is made up of 5 convolution layers.

For visual comparison, Figure 3 shows the DeepMRI reconstruction results with and without complex convolution. It can be seen that the reconstruction with complex convolution shows better performance, the error maps also indicate that network with complex convolution can achieve lower loss, which shows the importance of utilizing the complex convolution.

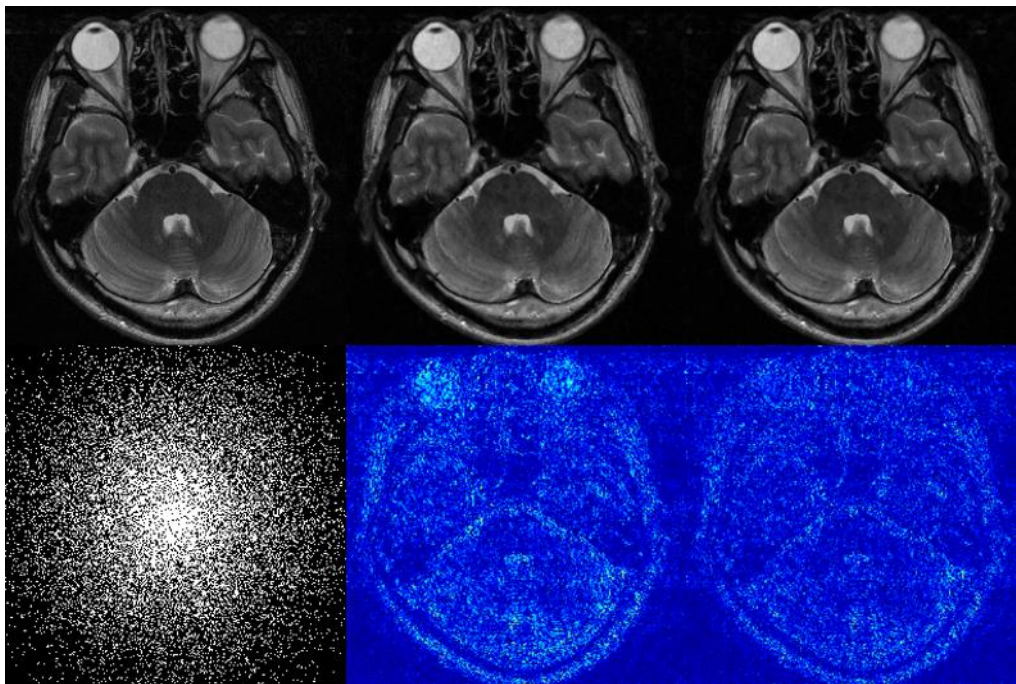


FIG. 3. DeepMRI reconstruction results with a 2D random undersampling pattern at an acceleration factor of 4. From left to right: ground-truth & mask, reconstruction without complex convolution and its corresponding error map, reconstruction with complex convolution and its corresponding error map.

We also show the comparison in Figure 4, the results of which give support for using complex convolution for DeepMRI based on PSNR and SSIM measures. This experiment was conducted

on 15 complex-valued brain MR images for testing by using a 2D random 25%-sampled mask. It can be observed that our DeepMRI with complex convolution outperforms the real convolution version of DeepMRI. Therefore, the test results in both visual and quantitative comparison demonstrated that complex convolution can help the network to obtain better image reconstruction results.

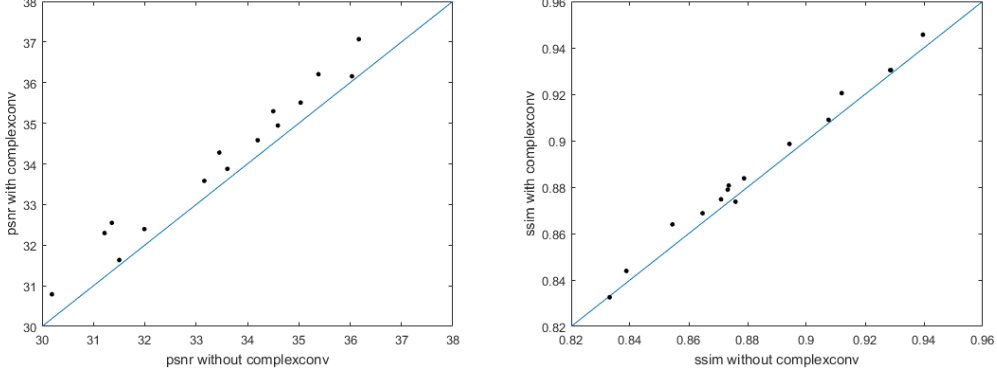


FIG. 4. A quantitative comparison of DeepMRI reconstruction results with and without complex convolution in PSNR and SSIM.

Comparison to state-of-the-art methods

To further evaluate the propose method, we compared our methods with two state-of-the-art methods SPIRiT and L1-SPIRiT with different undersampling patterns. SPIRiT and L1-SPIRiT adopted 1D random undersampling patterns with autocalibration lines and typical parameter settings. Specifically, the kernel size was 7×7 and calibration region had 24 lines for both. For SPIRiT, the iteration number was 30. As for the compressed sensing based parallel imaging technique L1-SPIRiT, Tikhonov regularization parameter was set as 0.01 and the Wavelet soft-thresholding regularization parameter was set as 0.015. It is worth noting that the proposed networks for all the later experiments consist of 10 blocks, and each block is made up of 5 complex convolution layers.

Figure 5 shows that the image reconstructed by SPIRiT, L1-SPIRiT and the proposed method at an acceleration factor of 3. It should be noted that it is a net acceleration factor with autocalibration lines calculated for the sampling rate. It can be observed that the images reconstructed by the proposed method is closer to the ground truth image, while there are aliasing artifacts in the images reconstructed by SPIRiT, L1-SPIRiT. The corresponding qualitative comparisons in error map are also shown in Figure 5. It could be observed that there are almost no error in our proposed method, while the other two methods show some noise and aliasing artifacts.

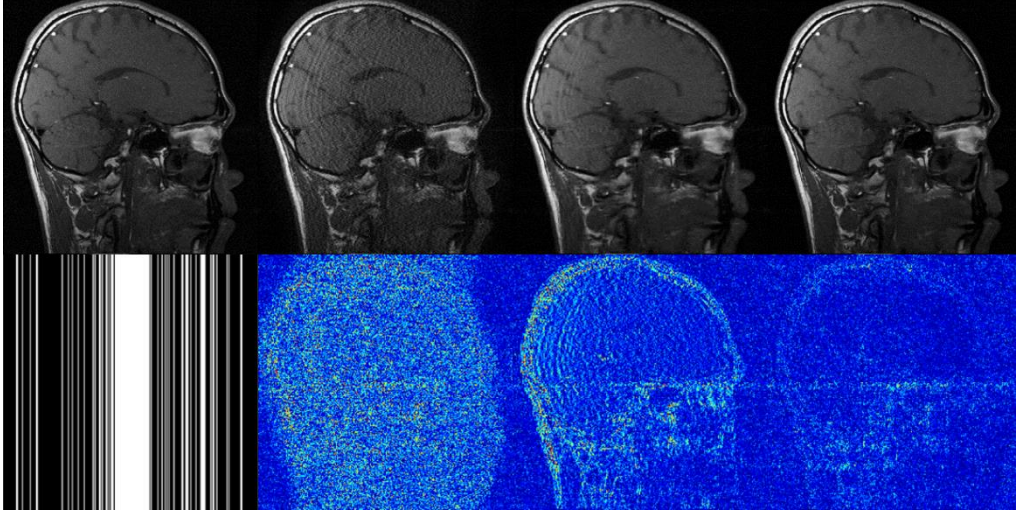


FIG. 5. From left to right: ground-truth & mask, the reconstruction of SPIRiT, L1-SPIRiT and proposed method with 1D random mask at a net acceleration of 3 (33% sampling).

To further validate our method with other sampling patterns, we have also investigated our method with the 2D Poisson undersampling mask. We trained networks with different acceleration factors with this sampling pattern. The reconstruction results have been provided in Figure 6. It demonstrates that the proposed method produced better visual quality with 2D Poisson disc masks at an acceleration factor of 3x. And with acceleration factors increasing from three to ten, the reconstruction gradually worsens. Nevertheless, the proposed method had a positive performance under 2D Poisson disc mask even at 10x acceleration. We can observe that the proposed network can learn valuable prior information from big off-line datasets, and then perform high-quality online image reconstruction from different undersampled MR data.

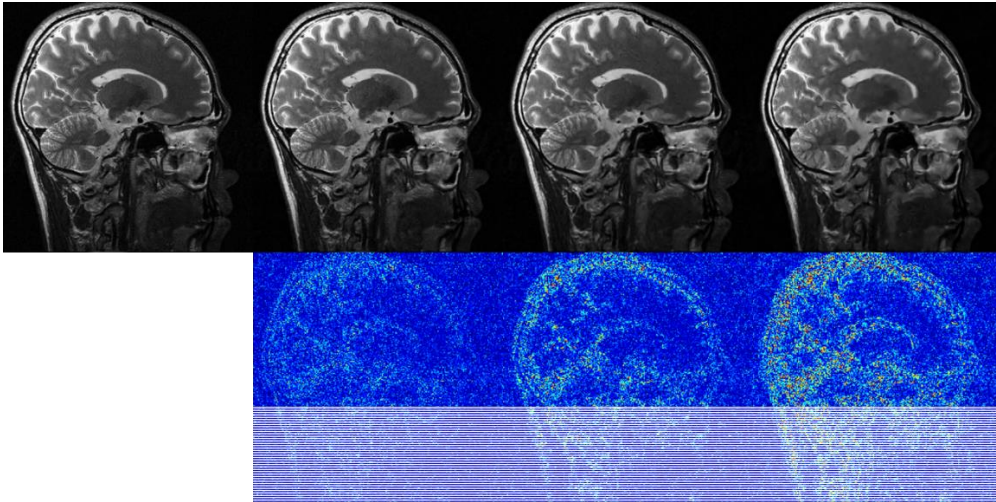


FIG. 6. From left to right: ground-truth, the reconstructions with 2D Poisson disc masks at acceleration factor of 3x, 5x, 10x and their corresponding error maps.

Combined-single-coil reconstruction vs multi-coil reconstruction

For parallel imaging, there could be another alternative that used the network to learn the mapping relationship between the Walsh adaptively combined images [44] reconstructed from

multi-coil undersampled and fully sampled measurements. We call it combined-single-coil reconstruction. Multi-coil reconstruction means we directly learn the mapping from undersampled multi-channel image to multi-channel fully sampled images. Figure 7 is a comparison of the results of the two methods. It can be seen that the details of multi-coil reconstruction are clearer. It is apparent that the multi-coil network achieves lower loss than the combined-single-coil reconstruction, demonstrating the multi-coil network can actually help the network converge to a better solution. The result of multi-coil network was slightly better than that of the combined-coil reconstruction because multi-coil network can extract more features and learn more information from multi-channel data instead of the combined data. It suggests that training a multi-coil network for parallel imaging is preferred.

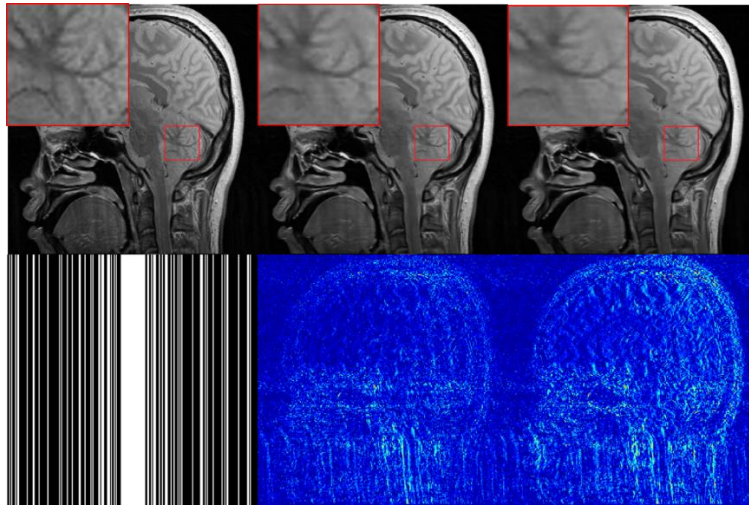


FIG. 7. A comparison of the groundtruth image (left), and the results with multi-coil reconstruction (middle) and combined-single-coil reconstruction (right)

Discussion

In this work, we exploit deep residual network for fast parallel MR imaging with complex convolution based on our previous research. A complex residual network is designed to train multi-coil parallel MR data. Residual connections can avoid the vanishing gradient problems and complex convolution can improve convergence ability of network and therefore contribute to learn a more accurate prior information. By comparing the experimental results in Figure 3 and Figure 4, we conclude that the deep residual learning network based on complex convolution can achieve better reconstruction quality.

Sensitivity to autocalibration lines

We all know that the mask used in classical SPIRiT and L1-SPIRiT algorithms requires acquisition of ACS lines. These classical methods are sensitive to the number of ACS lines, which actually increases the scanning time. Based on the observation from the ACS line and the above experiments, the proposed method shows better performance than other methods with 1D random mask at an acceleration factor of 3. And we performed another experiment with the same undersampling pattern at an even higher acceleration factor of 4x acceleration but with fewer autocalibration signal (ACS) line, namely 8 lines. The experimental results show that the reconstructed image is close to the reference image as shown in Figure 8. It is concluded that

the proposed method can still reconstruct high-quality images with high acceleration factors even with a few ACS lines. The sensitivity of the proposed methods to ACS line is relatively low.

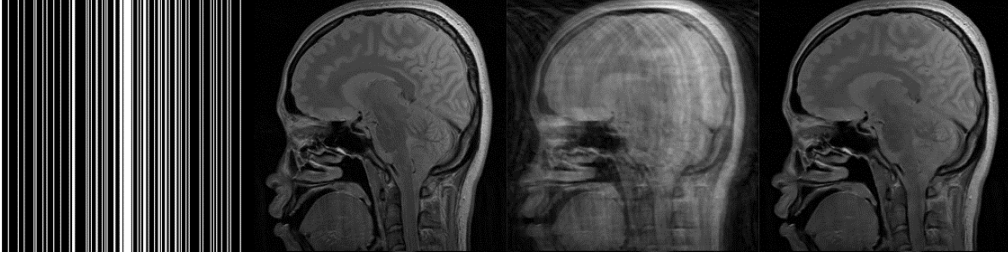


FIG. 8. From left to right: 1D random mask (AF=4, ACS=8), ground-truth, zero-filling image and reconstruction of the proposed method.

Convergence property

The performance of complex convolution can be evaluated using the above reconstruction result and the comparison of PSNR, SSIM. To have a better understanding about the performance of complex convolution, we analyze the proposed complex convolution from the error convergence property. Figure 9 plots the loss-descending curves of the training with and without complex convolution. As can be seen from the figure, our DeepMRI model reaches convergence after 40-epoch training. Furthermore, both the training loss and validation loss with complex convolution are lower than those of the model without complex convolution, which further demonstrates the impact of complex convolution. From the comparison, we claim that the improvement of the network convergence property is mainly attributed to the complex convolution. This is mainly because that complex convolution can fully leverage the magnitude and phase information based on parallel multi-coil data.

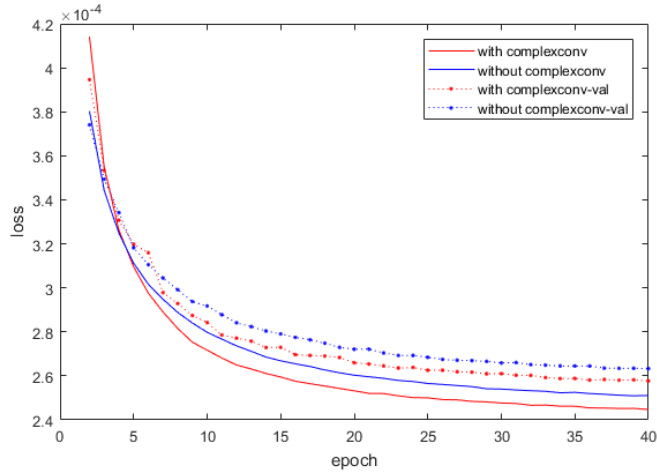


FIG. 9. The loss curve of the training with and without complex convolution.

Conclusion

This work designs and trains a deep residual network for parallel MR imaging. The network learns prior information from a huge set of existing high-quality fully-sampled multichannel data and then serves as a predictor to restore lost information in the undersampled multi-channel complex data. For the complex MR data, we also develop a complex convolution to improve the performance of the proposed network. The experimental results have shown that the

proposed method can produce images with less noise and artifacts than the classical SPIRiT, and L1-SPIRiT at the same 1D acceleration factor. It is worth mentioning that the proposed framework is flexible and extendable. Future work will further optimize the complex-valued networks and apply more training data for even faster MR imaging.

Acknowledgements

This research was partly supported by the National Natural Science Foundation of China (61601450, 61871371, 81830056, 61771463, 61471350), the Basic Research Program of Shenzhen (JCYJ20150831154213680), Key Laboratory for Magnetic Resonance and Multimodality Imaging of Guangdong Province (2017YFC0108802) and Science and Technology Planning Project of Guangdong Province(2017B020227012)

References

1. Pruessmann KP, Weiger M, Scheidegger MB, Boesiger P. *SENSE: sensitivity encoding for fast MRI*. Magnetic resonance in medicine 1999; **42**(5):952-962.
2. Sodickson DK, Manning WJ. *Simultaneous acquisition of spatial harmonics (SMASH): fast imaging with radiofrequency coil arrays*. Magnetic resonance in medicine 1997; **38**(4):591-603.
3. Griswold MA, Jakob PM, Heidemann RM, Nittka M, Jellus V, Wang J, Kiefer B, Haase A. *Generalized autocalibrating partially parallel acquisitions (GRAPPA)*. Magnetic resonance in medicine 2002; **47**(6):1202-1210.
4. Lustig M, Pauly JM. *SPIRiT: Iterative self-consistent parallel imaging reconstruction from arbitrary k-space*. Magnetic resonance in medicine 2010; **64**(2):457-471.
5. Uecker M, Lai P, Murphy MJ, Virtue P, Elad M, Pauly JM, Vasanawala SS, Lustig M. *ESPIRiT—an eigenvalue approach to autocalibrating parallel MRI: where SENSE meets GRAPPA*. Magnetic resonance in medicine 2014; **71**(3):990-1001.
6. Pruessmann KP, Weiger M, Börnert P, Boesiger P. *Advances in sensitivity encoding with arbitrary k-space trajectories*. Magnetic resonance in medicine 2001; **46**(4):638-651.
7. Weller DS, Polimeni JR, Grady L, Wald LL, Adalsteinsson E, Goyal VK. *Sparsity-promoting calibration for GRAPPA accelerated parallel MRI reconstruction*. Medical Imaging, IEEE Transactions on 2013; **32**(7):1325-1335.
8. Park J, Zhang Q, Jellus V, Simonetti O, Li D. *Artifact and noise suppression in GRAPPA imaging using improved k-space coil calibration and variable density sampling*. Magnetic resonance in medicine 2005; **53**(1):186-193.
9. Ramani S, Fessler JA. *Parallel MR image reconstruction using augmented Lagrangian methods*. IEEE transactions on medical imaging 2011; **30**(3):694-706.
10. Chaâri L, Pesquet J-C, Benazza-Benyahia A, Ciuciu P. *A wavelet-based regularized reconstruction algorithm for SENSE parallel MRI with applications to neuroimaging*. Medical image analysis 2011; **15**(2):185-201.
11. Block KT, Uecker M, Frahm J. *Undersampled radial MRI with multiple coils. Iterative image reconstruction using a total variation constraint*. Magnetic resonance in medicine 2007; **57**(6):1086-1098.

12. Osher S, Burger M, Goldfarb D, Xu J, Yin W. *An iterative regularization method for total variation-based image restoration*. Multiscale Modeling & Simulation 2005; **4**(2):460-489.
13. Chen C, Li Y, Huang J. *Calibrationless parallel MRI with joint total variation regularization*, in *Medical Image Computing and Computer-Assisted Intervention–MICCAI 2013*. 2013, Springer. p. 106-114.
14. Liang D, Wang H, Chang Y, Ying L. *Sensitivity encoding reconstruction with nonlocal total variation regularization*. Magnetic resonance in medicine 2011; **65**(5):1384-1392.
15. Weller D. *Reconstruction with dictionary learning for accelerated parallel magnetic resonance imaging*. in *2016 IEEE Southwest Symposium on Image Analysis and Interpretation (SSIAI)*. 2016. p. 105-108.
16. Liang Z-P. *Spatiotemporal imaging with partially separable functions*. in *4th IEEE International Symposium on Biomedical Imaging: From Nano to Macro*. 2007. p. 988-991.
17. Haldar JP, Zhuo J. *P-LORAKS: Low-rank modeling of local k-space neighborhoods with parallel imaging data*. Magnetic Resonance in Medicine 2016; **75**(4):1499-1514.
18. Kim TH, Setsompop K, Haldar JP. *LORAKS makes better SENSE: Phase-constrained partial fourier SENSE reconstruction without phase calibration*. Magnetic Resonance in Medicine 2017; **77**(3):1021-1035.
19. Shin PJ, Larson PE, Ohliger MA, Elad M, Pauly JM, Vigneron DB, Lustig M. *Calibrationless parallel imaging reconstruction based on structured low-rank matrix completion*. Magnetic resonance in medicine 2014; **72**(4):959-970.
20. Zhou Z, Wang J, Balu N, Li R, Yuan C. *STEP: Self-supporting tailored k-space estimation for parallel imaging reconstruction*. Magnetic resonance in medicine 2016; **75**(2):750-761.
21. Wu J, Liu F, Jiao L, Wang X, Hou B. *Multivariate compressive sensing for image reconstruction in the wavelet domain: Using scale mixture models*. IEEE Transactions on Image Processing 2011; **20**(12):3483-3494.
22. Wachinger C, Yigitsoy M, Rijkhorst E-J, Navab N. *Manifold learning for image-based breathing gating in ultrasound and MRI*. Medical image analysis 2012; **16**(4):806-818.
23. Nakarmi U, Wang Y, Lyu J, Liang D, Ying L. *A kernel-based low-rank (KLR) model for low-dimensional manifold recovery in highly accelerated dynamic MRI*. IEEE Transactions on Medical Imaging 2017; **36**(11):2297-2307.
24. Poddar S, Jacob M. *Dynamic MRI using smoothness regularization on manifolds (SToRM)*. IEEE transactions on medical imaging 2016; **35**(4):1106-1115.
25. Liang Z-P, Madore B, Glover GH, Pelc NJ. *Fast algorithms for GS-model-based image reconstruction in data-sharing Fourier imaging*. IEEE transactions on medical imaging 2003; **22**(8):1026-1030.
26. Samsonov AA, Kholmovski EG, Parker DL, Johnson CR. *POCSENSE: POCS - based reconstruction for sensitivity encoded magnetic resonance imaging*. Magnetic resonance in medicine 2004; **52**(6):1397-1406.
27. Chang Y, Liang D, Ying L. *Nonlinear GRAPPA: A kernel approach to parallel MRI reconstruction*. Magnetic resonance in medicine 2012; **68**(3):730-740.
28. Wang S, Su Z, Ying L, Peng X, Zhu S, Liang F, Feng D, Liang D. *Accelerating magnetic resonance imaging via deep learning*. in *IEEE 13th International Symposium on Biomedical Imaging (ISBI)*. Prague, Czech Republic, 2016. p. 514-517.
29. Wang S, Ying L, Peng X, Su Z, Liang D. *Exploiting deep convolutional neural network for*

- fast magnetic resonance imaging*. in *Proceedings of the 24th Annual Meeting of ISMRM*. Singapore, 2016. p. 1778.
30. Hammernik K, Klatzer T, Kobler E, Recht MP, Sodickson DK, Pock T, Knoll F. *Learning a variational network for reconstruction of accelerated MRI data*. *Magnetic resonance in medicine* 2018; **79**(6):3055-3071.
 31. Knoll F, Hammernik K, Kobler E, Pock T, Recht MP, Sodickson DK. *Assessment of the generalization of learned image reconstruction and the potential for transfer learning*. *Magnetic Resonance in Medicine* 2018. DOI: <https://doi.org/10.1002/mrm.27355>.
 32. Sun J, Li H, Xu Z. *Deep ADMM-Net for compressive sensing MRI*. in *Advances in Neural Information Processing Systems*. 2016. p. 10-18.
 33. Zhu B, Liu JZ, Cauley SF, Rosen BR, Rosen MS. *Image reconstruction by domain-transform manifold learning*. *Nature* 2018; **555**(7697):487.
 34. Han Y, Yoo J, Kim HH, Shin HJ, Sung K, Ye JC. *Deep learning with domain adaptation for accelerated projection - reconstruction MR*. *Magnetic resonance in medicine* 2018; **80**(3):1189-1205.
 35. Eo T, Jun Y, Kim T, Jang J, Lee HJ, Hwang D. *KIKI-net: cross-domain convolutional neural networks for reconstructing undersampled magnetic resonance images*. *Magnetic Resonance in Medicine* 2018. DOI: <https://doi.org/10.1002/mrm.27201>.
 36. Sun L, Fan Z, Huang Y, Ding X, Paisley J. *Compressed Sensing MRI Using a Recursive Dilated Network*. in *Association for the Advancement of Artificial Intelligence(AAAI)*. Arlington, Virginia, 2018.
 37. Quan TM, Nguyen-Duc T, Jeong W-K. *Compressed sensing MRI reconstruction using a generative adversarial network with a cyclic loss*. *IEEE transactions on medical imaging* 2018; **37**(6):1488-1497.
 38. Schlemper J, Caballero J, Hajnal JV, Price AN, Rueckert D. *A deep cascade of convolutional neural networks for dynamic MR image reconstruction*. *IEEE transactions on medical imaging* 2018; **37**(2):491-503.
 39. Qin C, Hajnal JV, Rueckert D, Schlemper J, Caballero J, Price AN. *Convolutional recurrent neural networks for dynamic MR image reconstruction*. *IEEE Transactions on Medical Imaging* 2018. DOI: 10.1109/TMI.2018.2863670.
 40. Lee D, Yoo J, Tak S, Ye JC. *Deep Residual Learning for Accelerated MRI using Magnitude and Phase Networks*. arXiv preprint arXiv:1804.00432 2018.
 41. Kwon K, Kim D, Park H. *A parallel MR imaging method using multilayer perceptron*. *Medical physics* 2017; **44**(12):6209-6224.
 42. Wang S, Ke Z, Cheng H, Ying L, Liu X, Zheng H, Liang D. *Investigation of convolutional neural network based deep learning for cardiac imaging*. in *26th ISMRM annual meeting*. Paris, France, 2018. p. 2786.
 43. Wang S, Cheng H, Ke Z, Ying L, Liu X, Zheng H, Liang D. *Complex-valued residual network learning for parallel MR imaging*. in *26th ISMRM annual meeting*. Paris, France, 2018. p. 2781.
 44. Walsh DO, Gmitro AF, Marcellin MW. *Adaptive reconstruction of phased array MR imagery*. *Magnetic Resonance in Medicine: An Official Journal of the International Society for Magnetic Resonance in Medicine* 2000; **43**(5):682-690.